JOURNAL OF GEOPHYSICAL RESEARCH, VOL. 112, B06314, doi:10.1029/2006JB004543, 2007

A global index earthquake approach to probabilistic assessment of extremes

Eric M. Thompson,[1] Laurie G. Baise,[1] and Richard M. Vogel[1]

Received 2 June 2006; revised 5 February 2007; accepted 20 March 2007; published 28 June 2007.

[1] This paper applies recent innovations in flood frequency analysis to regional series of earthquake magnitudes in the global Centroid Moment Tensor (CMT) catalog from 1976 to 2005. Probability plot correlation coefficient hypothesis tests and *L*-moment goodness-of-fit evaluations reveal that the Gumbel (GUM) distribution provides a good approximation to the probability distribution function (pdf) of series of annual maximum (AM) earthquake magnitudes. Homogeneity tests based on the theory of *L*-moments further reveal that broad regions of the globe are homogeneous in the sense that the AM observations of earthquake magnitudes are well approximated by a GUM pdf with fixed upper moments. The homogeneity of global earthquake data across broad tectonic environments enables us to pool data into a regional pdf of earthquake magnitudes, termed an index earthquake distribution. Research in hydrology has shown that frequency analysis based on pooling of data using an analogous index-flood method are much more accurate than frequency analysis based on site or region specific data. The index earthquake distribution is a dimensionless GUM distribution with fixed scale parameter so only the mean earthquake magnitude must be estimated for a region to define the frequency distribution of large earthquakes. We show how the degree of spatial homogeneity of earthquake magnitudes across broad tectonic environments can be exploited to yield improved estimates of the risk posed by extreme earthquake magnitudes.

Citation: Thompson, E. M., L. G. Baise, and R. M. Vogel (2007), A global index earthquake approach to probabilistic assessment of extremes, *J. Geophys. Res.*, *112*, B06314, doi:10.1029/2006JB004543.

1. Introduction

[2] The Gutenberg-Richter (GR) model [*Gutenberg and Richter*, 1954] is widely used and has been shown to fit both worldwide and regional earthquake catalogs. A review of the seismic literature demonstrates that many researchers have questioned the validity of the GR model [*Cosentino et al.*, 1977; *Dargahi-Noubary*, 1986; *Pacheco et al.*, 1992; *Main*, 1996; *Stein and Newman*, 2004]. Analogously, in the field of flood frequency analysis, the Gumbel (GUM) model [*Gumbel*, 1958] was once documented as the most widely used model of flood frequency (see *Cunnane* [1989] or the summary provided by *Vogel and Wilson* [1996]), until the introduction of the theory of *L*-moments [*Hosking*, 1990] and regional methods for pooling flood data [*Hosking and Wallis*, 1997].

[3] The theory of *L*-moments [*Hosking*, 1990] and regional methods for pooling flood data [*Hosking and Wallis*, 1987] have transformed hydrologic flood frequency analysis over the past few decades. *L*-moment diagrams enable an unbiased evaluation of the goodness-of-fit of alternate probability distribution functions (pdfs) to regional flood series and have proven to be an important improvement over traditional product moment diagrams in most instances [*Vogel and Fennessey*, 1993]. Dozens and possibly hundreds of studies around the world have now applied *L*-moment diagrams (there are over 270 citations to *Hosking* [1990]) to assess the goodness of fit of alternative distributions to flood series and other natural phenomena. As a result, by the end of the last century it has now become common practice to replace the GUM model with its three-parameter generalization known as the generalized extreme value (GEV) distribution to problems in flood frequency analysis [*Stedinger et al.*, 1993]. Similarly, it is now common practice in hydrology to pool information from many samples to improve the precision associated with estimates of flood frequency model parameters [*Hosking and Wallis*, 1987]; such methods are termed regional methods in hydrology. While these recent innovations have been applied to other natural hazards such as ocean wave heights [*Ma et al.*, 2006], wind speeds [*Cheng and Yeung*, 2002], and rainfall events [*Onibon et al.*, 2004], surprisingly few have been applied to earthquakes.

[4] Much of the discussion in the seismology literature concerning the limitations of the GR relationship for large events has focused on the characteristic earthquake model as the alternative [*Youngs and Coppersmith*, 1985; *Kagan*, 1993; *Stein and Newman*, 2004]. In support of the GR model, *Howell* [1985] demonstrated that the small sample size of large earthquakes will cause scatter in the large

[1]Department of Civil and Environmental Engineering, Tufts University, Medford, Massachusetts, USA.

0148-0227/07/2006JB004543$09.00

magnitude range of the data, which can be inappropriately used as evidence for the characteristic earthquake model. *Kagan* [1993] attributed the observed "evidence" of the characteristic earthquake to statistical bias and argued that the formulation of the characteristic model is so vague that it cannot be rigorously verified, and therefore supported simpler models. *Main* [2000] found that multiple slope GR models are not justified because the observed differences in recurrence rates for small and large earthquakes in the same region are not statistically different. *Stein and Newman* [2004] demonstrated that sampling bias and inaccurate paleoseismic estimates can result in data that mistakenly have the appearance of the characteristic earthquake model. The method of pooling data from different statistically homogeneous regions, commonly used in hydrology, can help overcome these problems by compensating for the small sample size of large events within individual regions.

[5] The application of the GR model to the series of earthquake magnitudes is equivalent to application of an exponential (EXP) pdf [*Kijko and Graham*, 1998; *Utsu*, 1999; *Lombardi*, 2003]. A number of alternative pdfs have been introduced for modeling earthquake magnitudes; in this paper we consider the class of extreme value distributions that have found common use in other applications of natural hazards such as the generalized Pareto (GP) and GEV pdfs. These distributions are commonly applied to floods, rainfall, wind speeds, wave heights, insurance pay outs, and other extremes; see *Beirlant et al.* [2005] for a review of different applications. The GEV distribution is a generalization of the three possible limit distributions known as the Extreme value type I (Gumbel), II (Frechet), and III (Weibull) distributions. *Makjanić* [1980, 1982] first introduced the GEV distribution to the field of seismology as an alternative to the GR model, but termed it a generalized exponential model. The GP pdf was first introduced to seismology by *Dargahi-Noubary* [1986] and was discussed more recently by *Pisarenko and Sornette* [2003]. In the field of flood frequency analysis, the GP and GEV pdfs have nearly replaced the more parsimonious GR/EXP and GUM pdfs over the past decade. One of the primary goals of this study is to evaluate the potential of the GP and GEV pdfs to model the frequency behavior of earthquakes.

[6] As in flood frequency analysis, we term the earthquake magnitude series above a threshold m_o as the peak over threshold (POT) series and the series of the largest earthquake magnitude per year in a region as the annual maximum (AM) series. Many researchers [*Epstein and Lomnitz*,1966; *Rosbjerg et al.*,1992; *Stedinger et al.*,1993; *Lombardi*, 2003; and others] have shown that a GR/EXP model of the POT series is equivalent to a GUM model of the AM series assuming a Poisson distribution of earthquake arrival times. The generalized form of the GR/EXP, termed the GP distribution provides a more flexible model of extremes above a threshold [*Embrechts et al.*, 1997]. Similarly, research in other fields of natural hazard frequency analysis has shown that the GEV, a generalized form of the GUM model, provides a much more flexible model of AM records than the GUM model.

[7] In the past, the parameters of flood frequency probability models were estimated from only the data available for a particular river. These "at-site" flood samples were often too short to provide reliable estimates of large floods. For this reason, hydrologists have incorporated alternative sources of information, including the pooling of samples over space to compensate for short record lengths. One such regional pooling method, termed the index-flood method, has been shown to be reasonably robust and more accurate than at-site methods which estimate two or three parameters of a pdf at a single site [*Potter*, 1987; *Bobee and Rasmussen*, 1995]. Another goal of this study is to document how recent developments in the field of regional flood frequency analysis [*Stedinger et al.*, 1993; *Hosking and Wallis*, 1997] may offer valuable alternatives to the traditional use of earthquake records from a single location.

[8] We begin by summarizing the various probability distributions and associated parameter estimation algorithms that we consider as potential models for earthquake magnitudes. For clarity, the probability distributions and parameter estimation algorithms are given in Appendices A and B, respectively. We then present the *L*-moment diagrams, which provide a unique summary of the distributional properties of the global earthquake catalog. These diagrams motivate the application of numerous heterogeneity hypothesis tests in the subsequent section. On the basis of the results of those heterogeneity tests and the assumption of the GUM pdf, we conclude by illustrating the advantages of fitting a global index earthquake distribution.

2. Probability Distributions and Parameter Estimation

[9] In hydrology, it is now standard practice to fit a probability distribution to the AM series of floods rather than the POT series, which is the series of floods above a threshold [*Stedinger et al.*, 1993; and many others]. Although both the POT and AM approaches have been used in hydrology, common flood design practices employ the AM series. *Rosbjerg et al.* [1992] and *Stedinger et al.* [1993, chapter 18.6.1] provide a discussion of the advantages and disadvantages of each approach and describe the theoretical relationships between both series. When working with the POT series of earthquake magnitudes, one needs to combine the fitted pdf of earthquake magnitudes (i.e., GR/EXP or GP models), with a probabilistic model of earthquake arrivals. The Poisson distribution is the simplest and most commonly applied pdf, although earthquake arrival times exhibit persistence. *Rosbjerg et al.* [1992] and *Stedinger et al.* [1993] show that the use of the EXP/GR model for modeling the POT series combined with a Poisson model of earthquake or flood arrivals is equivalent to modeling the AM series using a GUM pdf. The advantage to working with the POT series is that it includes a much larger number of observations; the disadvantage is that the assumption of independence cannot be justified. *Rosbjerg et al.* [1992], *Stedinger et al.* [1993], and others have shown that if one combines a GP model of the POT series with a Poisson model of arrival times, then the AM series is GEV. Thus an EXP/GR model of earthquake POT series is equivalent to a GUM model of the AM series of earthquake magnitudes and a GP model of the earthquake POT series is equivalent to a GEV model of the AM series. Relationships among the distributions fit to the POT and AM series pdfs are given in Appendix A.

[10] A variety of methods are available for estimating the parameters of the pdfs considered for the POT and AM series.

The short length of individual flood and earthquake records causes estimation of extreme events to be unreliable. For this reason, hydrologists usually pool information from many data sets, substituting space for time to compensate for the short length of individual data sets. We use the term "index earthquake distribution" to describe this pooling method, which has proven to be an efficient approach in flood frequency analysis [*Dalrymple*, 1960; *Potter*, 1987; *Stedinger et al.*, 1993; *Hosking and Wallis*, 1997].

[11] In Appendix B, we describe the use of the method of moments (MM) for estimating the parameters of the four pdfs considered for modeling AM and POT series. We employ MM estimators instead of maximum likelihood (ML) estimators because a number of studies have shown that MM estimators are more efficient and less biased than either ML or *L*-moment [*Hosking*, 1990] estimators for the small samples which are normally encountered in AM series of earthquakes and floods. For example, *Hosking and Wallis* [1987] show that unless the sample sizes are above 500, MM and *L*-moment estimators are both more efficient than ML estimators. Similarly, *Madsen et al.* [1997] show that the MM estimators lead to more efficient quantile estimates for the GEV pdf than either the method of *L*-moments or ML for $-0.25 \leq \kappa \leq 0.3$ and sample sizes $n = 10-50$. *Christopeit* [1994] has shown that the MM provides reasonable GEV parameter estimates for the distribution of earthquake magnitudes. *Stedinger et al.* [1993] reviews the most efficient parameter estimation procedures for each of the models introduced above in the context of flood frequency analysis. In this initial paper, we employ MM estimators because they are efficient for the GP and GEV models for small samples, and they provide the most straightforward approach for introducing the index earthquake method. Appendix B introduces MM estimators of the parameters of the GR, EXP and GP models based on POT series and estimators of the parameters of the GUM and GEV models based on AM series.

3. *L*-Moment Diagrams for Distribution Selection

[12] An increasingly popular approach for assessing the goodness-of-fit of a particular probability distribution to observations of extreme events involves the construction of *L*-moment ratio diagrams, introduced by *Hosking* [1990]. *L*-moments are analogous to conventional product moments, but are estimated using linear combinations of the ordered observations. The *L*-moment ratios $L-C_v$, $L-$Skewness, and $L-$Kurtosis are analogues of the conventional moment ratios coefficient of variation C_v, skewness γ, and kurtosis K; *L*-moment diagrams are now used routinely in hydrology and meteorology, and increasingly in other fields. Moment ratio diagrams are constructed by plotting estimated moment ratios versus each other: for example, C_v versus γ, or K versus γ. On the same plot, the theoretical relationships for various pdfs are compared to the observations. *Vogel and Fennessey* [1993] have shown that *L*-moment diagrams are nearly always an improvement over ordinary product moment diagrams because *L*-moment ratios are approximately unbiased, whereas ordinary moment ratios can exhibit enormous downward bias, particularly for skewed samples, even with extremely large samples. *Chowdhury et al.* [1991], *Stedinger et al.* [1993], *Hosking and Wallis* [1997], and many others have summarized the theory of *L*-moments, so we do not reproduce that theory here. Instead, we simply report the resulting *L*-moment diagrams for a global data set of earthquake magnitudes in Figure 1. Here *L*-moments are computed using the software package "lmomco" [*Asquith*, 2006] in the open-source statistical computing language R [*R Development Core Team*, 2006].

[13] We calculate the POT and AM series *L*-moments of the moment magnitude, M_w, from the moment tensor solutions in the global CMT catalog [*Ekström et al.*, 2005] from 1 January 1976 to 31 December 2005. The scalar seismic moment (M_0) is reported in units of dyne-centimeter to four significant figures. From this value we calculate the moment magnitude $M_W = (2/3)*(\log(M_0) - 16.1)$ [*Kanamori*, 1977]. We adopt the magnitude of completeness of $m_o = 5.8$ that *Kagan* [1997] showed to be appropriate for this catalog. We test the assumption that the AM series in each region are independent in time, by performing a hypothesis test based on the lag-one serial correlation coefficient, $r(1)$, for the 16 regions that have uncensored AM series. Under the null hypothesis of independence, one expects $\mathrm{Var}[r(1)] = n^{-1/2}$ where n is the AM series record length. Using a 5% level test, the estimated values of $r(1)$ were all statistically indistinguishable from zero.

[14] Each point in Figure 1 represents the *L*-moment ratios for one of the 50 Flinn-Engdahl (FE) seismic geographic regions [*Young et al.*, 1996] illustrated in Figure 2. For the AM series we exclude 5 of the 50 FE regions from our analysis because those regions contain less than five earthquakes greater than or equal to magnitude 5.8. Figure 1a plots the *L*-moment ratio diagrams for the POT series. The $L-C_v$ versus $L-$Skewness plot includes the theoretical relationship for the EXP pdf and the plot of $L-$Kurtosis versus $L-$Skewness includes the theoretical relationship for both the EXP and GP pdfs. The record length weighted global average value of the *L*-moment ratios is also plotted in each figure for comparison with the theoretical values. Figure 1b compares the *L*-moment ratio diagrams for the AM series with theoretical relationships for the GUM and GEV distributions. Figure 1 illustrates a notable global homogeneity among values of $L-C_v$ for both the AM and POT series. This homogeneity is especially remarkable when compared to *L*-moment diagrams of floods and other natural phenomena summarized elsewhere [*Vogel and Wilson*, 1996; *Onibon et al.*, 2004; *Ma et al.*, 2006]. This remarkable homogeneity led us to the hypothesis, tested in a subsequent section, that the entire globe is homogeneous in terms of the upper moment ratios of earthquake magnitudes.

[15] Figure 1 qualitatively demonstrates that the record length weighted global mean *L*-moments are not significantly different than the theoretical values for a GUM pdf. This result led us to hypothesize that all of the earthquake series may arise from a single regional GUM pdf with a fixed global value of $L-C_v$. This hypothesis implies that the GEV distribution may not be necessary to model the frequency behavior of earthquake magnitudes.

4. Heterogeneity Tests and Identification of Homogeneous Regions

[16] A homogeneous group of samples is defined as a group whose frequency distribution (after appropriate scaling) is

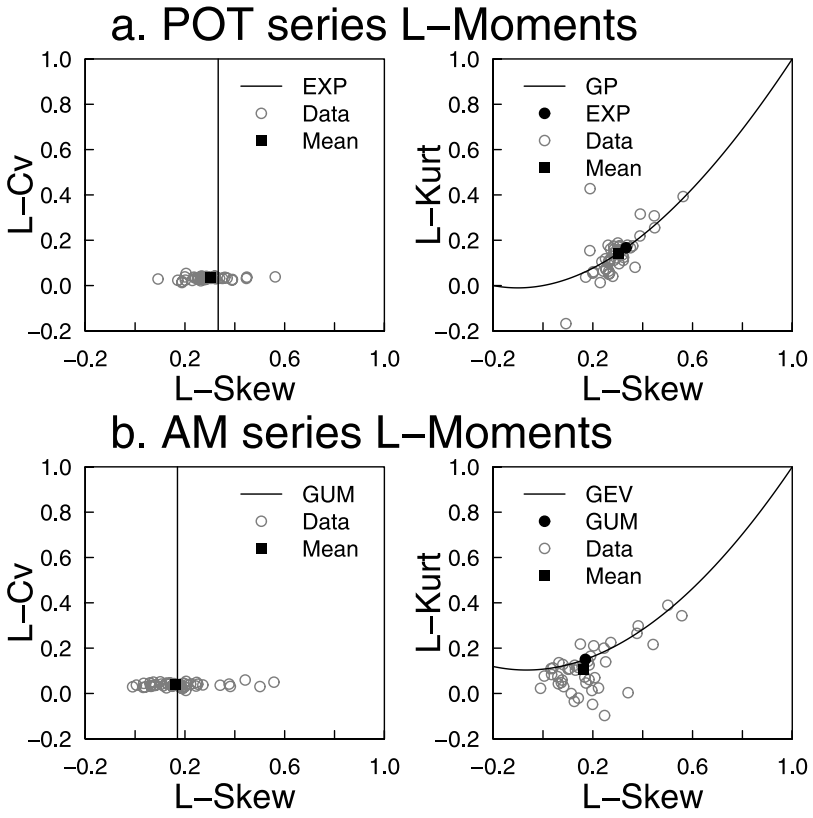

Figure 1. *L*-moment diagrams for the observed POT and AM series of earthquake magnitudes.

considered to be approximately the same. Showing that a group of samples is approximately homogeneous is sufficient to ensure that pooling of the samples will lead to a regional frequency analysis which is more accurate than using individual samples [*Hosking and Wallis*, 1997]. In hydrology, homogeneity is often judged by assessing the variability among the coefficient of variation, C_v, and/or skewness, γ (or their *L*-moment counterparts), of individual flood series records. The analog here would be to assess the variability of those same statistics among regional samples of earthquake series. In this section we evaluate homogeneity of earthquake samples using Monte Carlo simulation experiments and using analytical

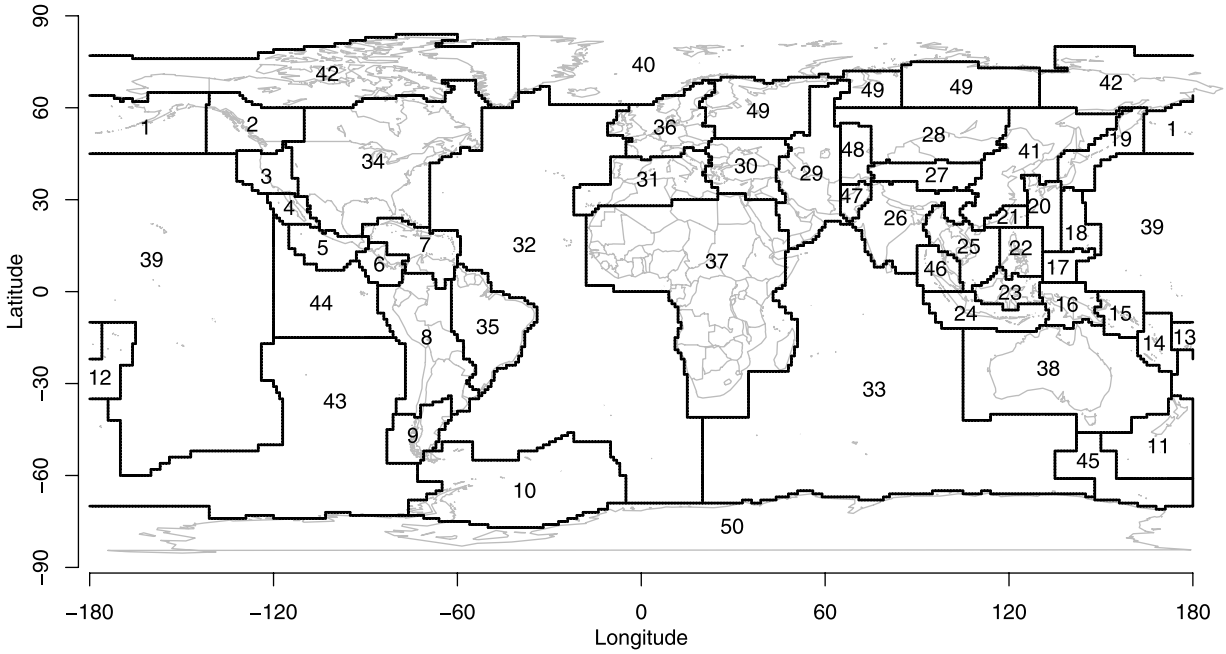

Figure 2. Map showing the boundaries of the Flinn-Engdahl Seismic Regions [*Young et al.*, 1996].

Table 1. Regional Heterogeneity Measure

Seismic Region Name	Number of FE Regions Included	H
Global Catalog	45	3.02
Subduction Zones[a]	18	3.16
Collision Zones[a]	10	−1.06
Intracontinental Regions[a]	3 (8)	0.96
Mid-Ocean Ridges[a]	7	1.19
Other[a]	7	1.66
E Subduction Zones	4	0.85
NW Subduction Zones	7	0.99
SW Subduction Zones	7	3.60
Subduction Zones, Collision Zones, and Intracontinental Regions	31	1.86
E and NW Subduction Zones, Collision Zones, and Intracontinental Regions	24	−0.02
E and NW Subduction Zones, Collision Zones, Intracontinental Regions, and Other	31	0.59

[a]Regions defined by *Kagan* [1997].

hypothesis tests introduced by *Hosking and Wallis* [1997] and others.

[17] *Hosking and Wallis* [1997] introduced a heterogeneity test statistic, H, based on the theory of L-moments. Computation of H, involves the use of Monte Carlo experiments which enable a comparison of the variability of individual sample estimates of $L-C_v$ with estimates based on the null hypothesis that earthquake magnitudes originate from a single homogeneous global index earthquake distribution with fixed regional $L-C_v$. *Hosking and Wallis* [1997] suggest that regions can be classified as "acceptably homogeneous" if $H < 1$, "possibly heterogeneous" if $1 < H < 2$, and "definitely heterogeneous" if $H > 2$. We used the implementation of this method within the R-project [*R Development Core Team*, 2006] by the package "RFA" [*Ribatet*, 2005].

[18] Table 1 summarizes the values of the homogeneity test statistic H for various combinations of seismic regions. We remove five intracontinental regions from the analysis because they lack sufficient data. The resulting global catalog of 45 regions yields a value of $H = 3.02$ indicating that the entire globe is "definitely heterogeneous" in the sense of the GUM hypothesis with fixed global $L-C_v$.

[19] We next explore whether smaller earthquake regions may be approximated as homogeneous. We hypothesize that the most physically plausible homogeneous regions for earthquakes should be defined by tectonic environment, since other researchers have found that the GR "*b* value" varies systematically for different styles of faulting [*Schorlemmer et al.*, 2005]. We combine FE regions to form larger regions based on tectonic environment as defined by *Kagan* [1997]. Table 1 indicates that collision zones (CZ) and intracontinental regions (IC) are homogeneous, while mid-ocean ridges (MOR) and others are possibly heterogeneous and subduction zones (SZ) are clearly heterogeneous.

[20] Because SZ contain a large portion of the catalog and produce the largest recorded earthquakes, we further investigate the heterogeneity of these regions by subdividing SZ into three regions based on geographic location. The eastern (E) and northwest (NW) SZ regions are homogeneous, yet the southwest (SW) SZ regions are heterogeneous. The SW SZ contain the recent M_W 9.0 Sumatra-Andaman earthquake which is the largest event in the catalog. This result either implies the region is heterogeneous or that perhaps a more flexible model such as the GEV model is needed to model earthquakes in the Andaman Island-Sumatra region.

[21] We further combine regions to explore the possibility that broad regions of the globe are homogeneous in the sense of the GUM hypothesis of earthquake magnitudes. We find that the super region that includes SZ, CZ, and IC regions is possibly heterogeneous. If we restrict the SZ to only the E and NW SZ regions that we previously showed to be homogeneous then the combined regions behave as a homogeneous super region.

[22] The heterogeneity of the FE regions described as "other" in Table 1 is inconclusively described as possibly heterogeneous. We add those FE regions to the E and NW SZ, CZ, and IC regions, and test the resulting super region; this super region is homogeneous, and contains 31 of the original 45 FE regions. The FE regions not included in this super region, the most inclusive of the conglomerated regions, are the SW SZ and the MOR regions.

[23] In addition to the above Monte Carlo simulation based tests of homogeneity we use the analytic homogeneity tests introduced by *Chowdhury et al.* [1991] and others. These tests evaluate the hypothesis that the dispersion of the L-moment statistics arise only from the variability produced by estimating the statistics from finite samples of a theoretical GUM pdf with a constant global average $L-C_v = 0.0402$ (illustrated in Figure 1). Note that a GUM pdf always exhibits a fixed $L-$Skewness and $L-$Kurtosis. Under the null hypothesis of a global GUM pdf with fixed global $L-C_v$, the only parameter that can vary from region to region is the mean of the AM series.

[24] *Dalrymple* [1960] first introduced a homogeneity test for the GUM pdf with more recent improvements introduced by *Chowdhury et al.* [1991], *Fill and Stedinger* [1995], and *Hosking and Wallis* [1997]. *Hosking* [1990] showed by simulation that a normal approximation for the distribution of sample estimates of $L-$Skew is excellent when samples are drawn from a GUM pdf. *Chowdhury et al.* [1991] use the normal approximation of $L-$Skew estimates to develop both an $L-C_v$ and $L-$Skew test for the GUM pdf. The two test statistics $Z = [\hat{\tau}_2 - \tau_2]/\sigma_{\hat{\tau}_2}$ and $Z = [\hat{\tau}_3 - \tau_3]/\sigma_{\hat{\tau}_3}$ follow a standard normal distribution, denoted $N(0,1)$. Here τ_2 is the global mean value of $L-C_v$, $\tau_3 = 0.1699$ for a GUM pdf, $\hat{\tau}_2$ $\hat{\tau}_3$ are the estimated values of $L-C_v$ and $L-$Skew for a particular region and $\sigma_{\hat{\tau}_2}$ and $\sigma_{\hat{\tau}_3}$ are the standard deviations of $\hat{\tau}_2$ and $\hat{\tau}_3$ reported in equations (16) and (17) of *Chowdhury et al.* [1991]. Since *Chowdhury et al* [1991] only reports values of $\sigma_{\hat{\tau}_2}$ for values of $\tau_2 \geq 0.1$, we prefer the equation $\sigma_{\hat{\tau}_2} = \sqrt{0.0883(\tau_2/0.4)^2/n}$ for $0 \leq \tau_2 \leq 0.4$ (J.R. Stedinger, personal communication, 2007).

[25] Figure 3 compares the test statistic Z corresponding to both the $L-C_V$ and $L-$Skew tests to a standard normal distribution. Here Z is computed for the original 45 FE regions as well as the super region containing only 31 of the original FE regions. Figure 3 demonstrates that both test statistics are well approximated by the $N(0,1)$ distribution.

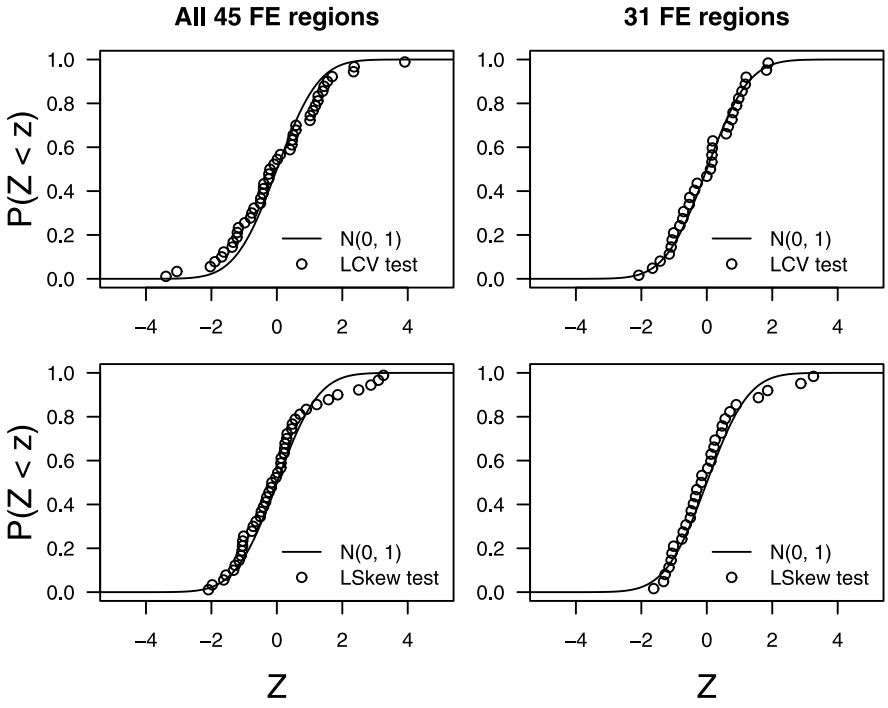

Figure 3. Comparison of the distribution of the *Chowdhury et al.* [1991] $L-C_v$ and $L-$Skew Test Statistics for the 31 and 45 FE regions with a standard normal distribution.

As expected from our previous results using the H statistic, the test statistic Z computed for the super region based on 31 FE regions, more closely resembles a $N(0,1)$ distribution than the test statistic Z computed for the original 45 FE regions. *Chowdhury et al.* [1991] found the $L-C_v$ test for the GUM pdf to be more powerful than the Kolmogorov-Smirnov test at detecting $L-C_v$ inconsistencies. Several other attractive tests of homogeneity are provided by *Chowdhury et al.* [1991] which we hope will be considered in future studies.

[26] We conclude that although the entire globe is not homogeneous in the sense of the GUM hypothesis with a fixed global value of $L-C_v$, Table 1 and Figure 3 document that broad regions of the globe are homogenous and that the approximation of homogeneity for the entire globe may be an adequate approximation. In flood frequency analysis, it is rare to find even a small geographic region that is homogeneous (for example, the size of a small state such as Rhode Island) so the degree of spatial homogeneity reported in Table 1 and Figure 3 for earthquake magnitudes across broad regions of the globe is striking and warrants further research.

5. Probability Plot Correlation Coefficient Hypothesis Tests

[27] While numerous hypothesis tests are available for testing alternative distributional hypotheses such as the Kolmogorov-Smirnov test and the Chi-square test, research has shown that the probability plot correlation coefficient (PPCC) test is more powerful than either of these tests for testing a number of extreme value distributional alternatives [*Stedinger et al.*, 1993; *Chowdhury et al.*, 1991]. For example, the PPCC test of normality compared favorably with seven other tests of normality on the basis of empirical power studies performed by *Filliben* [1975]. Since *Filliben* [1975], the PPCC test has been extended to dozens of other distributions. For example, *Vogel* [1986] and *Chowdhury et al.* [1991] developed critical values of the PPCC test statistic for the GUM and GEV distributions. The PPCC test is an attractive hypothesis test because it is based on the probability plot, which is a widely used graphical aid. The PPCC is simply a measure of the linearity of the probability plot. In this section we use the PPCC hypothesis test to evaluate the overall goodness-of-fit of the GUM pdf to each region in the global earthquake catalog.

[28] Values of the GUM PPCC for each of the 45 FE earthquake regions were compared to the critical values reported in *Vogel* [1986; Table 2] assuming a 5% significance level. When a computed value of PPCC exceeds the critical values reported, the GUM hypothesis is accepted at that significance level. Using a 5% significance level test, under the GUM null hypothesis one expects $0.05(45) = 2.25$ regions to have PPCC values below the reported critical values. While the power of individual hypothesis tests is low, the power associated with 45 individual hypothesis tests in this case is much higher. Repetitive implementation of the same test 45 times would be termed a field significance level test and such tests have been shown to be quite powerful [*Livezey and Chen*, 1983]. In our case, of the 45 regions, the GUM PPCC test was only rejected for three regions. Using a binomial test there is a 19% chance of getting three or more rejections out of 45 independent 5% level tests, thus the field significance is 19%. On the basis of these results we are unable to reject the GUM hypothesis for earthquake magnitudes for the entire global data set.

[29] We also computed the GUM PPCC test statistic for the 31 FE regions that were determined to be homogeneous in the previous section. For the 31 FE regions one would expect to reject the GUM null hypothesis for $0.05(31) = 1.55$ regions

Table 2. The Index Earthquake Distribution

FE Region Number	n	m_k	m (0.99)
NW Subduction Zones			
1	29	6.9	8.4
19	30	7.1	8.7
18	29	6.6	8.1
20	26	6.3[a]	7.7
21	27	6.5	7.9
22	30	7.0	8.5
23	30	6.8	8.3
E Subduction Zones			
5	30	6.8	8.3
6	30	6.7	8.1
7	24	6.2[a]	7.5
8	30	7.3	8.8
Collision Zones			
25	14	5.9[a]	7.2
26	25	6.2[a]	7.6
27	19	6.1[a]	7.4
28	7	5.5[a]	6.7
29	24	6.5[a]	7.9
30	26	6.4[a]	7.8
31	16	5.9[a]	7.2
41	24	6.3[a]	7.7
47	8	5.5[a]	6.7
48	28	6.4	7.8
Intracontinental Regions			
34	7	5.6[a]	6.8
37	17	6.0[a]	7.3
42	5	5.8[a]	7.1
Other			
2	15	5.9[a]	7.2
3	20	6.3[a]	7.7
9	16	5.9[a]	7.2
10	30	6.4	7.8
11	25	6.6[a]	8.0
17	15	5.9[a]	7.2
39	9	5.8[a]	7.0

[a]These values are censored maximum likelihood estimates [*Leese*, 1973].

yet only one of these FE regions had to be rejected. Using a binomial test there is a 46% chance of at least one rejection at the 5% significance level.

6. The Global Index Earthquake Distribution

[30] In hydrology, the pooling of samples, which is termed "regional frequency analysis", has long been preferred to the use of a single data series, except in rare cases when one has an extremely long record. It is now common practice in hydrology to pool summary statistics from different samples collected in a region to create a regional frequency distribution, rather than using a single sample to fit the frequency distribution. The most common method for pooling flood data series is termed the "index flood" method [*Dalrymple*, 1960] though in principle the method can be applied to other problems [e.g., *Ma et al.*, 2006; *Onibon et al.*, 2004]. When applied to earthquake data, we term the method an "index earthquake" method. *Stedinger et al.* [1993] and *Hosking and Wallis* [1997] summarize the most common regional approaches in hydrology with special emphasis given to the index flood method because it has proven to be one of the most robust and efficient methods available.

[31] The key assumption of an index earthquake method is that the r individual earthquake regions form an overall homogeneous super region; that is, the frequency distribution of the regions are identical, apart from a region-specific scaling factor termed the index earthquake. Thus

$$m_k(p) = \mu_k \cdot m_S(p) \tag{1}$$

where μ_k is the index earthquake in region k, which is simply the mean of the AM series of earthquake magnitudes in region k, $m_k(p)$ is the pth quantile of earthquake magnitudes in region k, and $m_S(p)$ is the super region quantile function, which is a normalized frequency distribution for the entire super region made up of individual regions. Here p is the nonexceedance probability given by the cumulative density function (cdf) $p = P[M \leq m]$ where M is the random variable earthquake magnitude and m is a realization of that variable.

[32] Normally, the index flood method is implemented using either probability weighted moments or L-moments, however, since these methods are not common in the seismic literature we introduce the "index earthquake" method using ordinary product moments. The resulting index earthquake model is a single GUM model with fixed parameters for the entire super region. Our approach, described below, refers to the theoretical development of the GUM pdf and method of moments estimators of its parameters that are summarized in Appendices A and B, respectively:

[33] 1. For each earthquake region $k = 1,\ldots,r$, compute the mean $\overline{m}_k$ and standard deviation s_k of the AM earthquake magnitudes from equation (B1) but with m_i equal to the AM earthquake magnitude in year i.

[34] 2. To obtain the normalized frequency distribution for the super region based on r individual regions, estimate a record length weighted value of the standard deviation of earthquake magnitudes for the super region using

$$s_S = \frac{\sum_{k=1}^{r} \frac{n_k s_k}{\overline{m}_k}}{\sum_{k=1}^{r} n_k} \tag{2}$$

[35] 3. Use the normalized moment estimates $\overline{m}_S = 1$ and s_S in place of $\overline{m}$ and s in equations (B4) and (B5) to obtain super region estimates of the GUM model parameters, which we term $\hat{\beta}_S$ and $\hat{\xi}_S$. The normalized quantile function for the super region consisting of r regions (also termed the index earthquake distribution) can be found by combining the quantile function of a GUM variable in equation (A22) with the estimators of $\hat{\beta}_S$ and $\hat{\xi}_S$ in equation (B4) with the fact that $\overline{m}_S = 1$ leading to the normalized GUM index earthquake quantile function

$$m_S(p) = 1 - \frac{[\ln(-\ln(p)) + \gamma] s_S \sqrt{6}}{\pi} \tag{3}$$

where $\gamma = 0.5772\ldots$ is the Euler-Mascheroni constant and s_S is defined in equation (2). We have changed the notation $m_{GUM}(p)$ used in equation (A22) in Appendix A, in order to emphasize here that the resulting GUM quantile function in equation (3) applies to the entire super region.

[36] 4. Now an estimate of the 100p percentile of the distribution of earthquake magnitudes for a particular

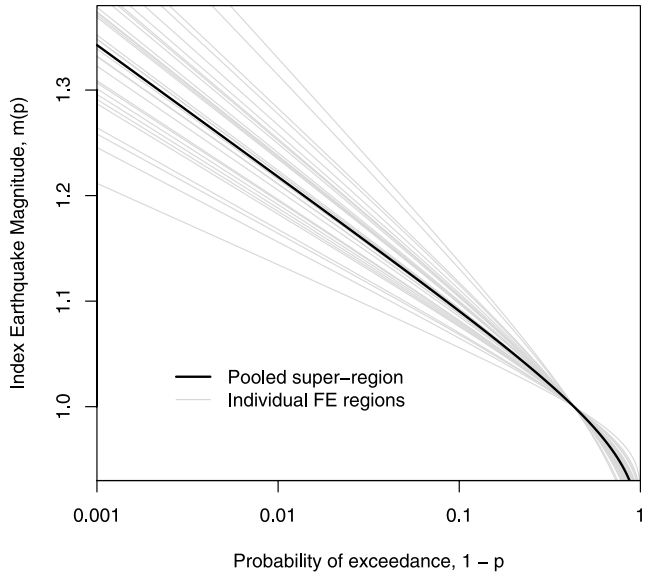

Figure 4. The index earthquake magnitude plotted as a function of the probability of exceedance. The bold line is the index earthquake magnitude for the super-region, $m_s(p)$, containing 31 FE seismic regions. The thin grey lines represent the equivalent earthquake magnitude based on the parameter estimates for each of the individual $k = 31$ FE regions.

region k (within the super region defined in equation (3)) is given by

$$m_k(p) = \overline{m}_k \cdot m_S(p) \tag{4}$$

where $m_S(p)$ is given in equation (3) and $\overline{m}_k$ is the mean earthquake magnitude for region k.

[37] For the super region with 31 FE regions, the standard deviation of earthquake magnitudes $s_s = 0.0694$. Table 2 summarizes the index earthquake distribution for FE regions within this super region by reporting the number of observations, n, the mean magnitude, $\overline{m}_k$, of the AM series for each region and the 100-year ($p = 0.99$) earthquake magnitude, $m_k(0.99)$ estimated from our GUM index earthquake model in equation (4). There is a slight complication with use of standard MM or ML estimators for the GUM parameters for some of the earthquake regions considered, because some earthquake records are censored samples. Although the record lengths are all 30 years, in some regions there are years in which no earthquake larger than the magnitude of completeness ($m_0 = 5.8$) occurred, thus those years are censored, reducing the sample size. We address this issue by applying a ML estimate of GUM parameters derived for censored observations [*Leese*, 1973] for the 20 regions in which the censoring is greater than 10%. We could not find a MM estimator for censored samples for the GUM distribution. Since this censoring issue is so important for the frequency analysis of earthquakes, further research is needed to address this issue.

[38] Figure 4 plots the earthquake magnitude, $m_s(p)$, as a function of its probability of exceedance. The bold curve is the index earthquake magnitude for the super region, $m_s(p)$, and the thin grey curves represent the equivalent earthquake magnitude based on the parameter estimates for each of the individual $k = 31$ FE regions. If data were not pooled across the different FE regions as in the index earthquake model (given by the bold curve in Figure 4), the quantiles of earthquake magnitudes would be estimated by the various thin grey curves in Figure 4. Estimates of the 100-year earthquake based on the individual regional quantile functions (shown by thin grey curves) would have much greater sampling variability than estimates of 100-year earthquakes based on the index earthquake model introduced here. This has been proven for the analogous flood estimates by dozens of previous regional studies available in the literature on regional flood frequency analyses (summarized by *Stedinger et al.* [1993] and *Hosking and Wallis* [1997]).

7. Conclusion

[39] Many statistical methods introduced to the field of hydrologic frequency analysis are now considered standard practice in the field of mathematical statistics as evidenced by their inclusion in the "Encyclopedia of Statistical Sciences" [e.g., *Hosking*, 1998]. There has been an evolution in the field of flood frequency analysis from use of the EXP and GUM models of POT and AM series, respectively, several decades ago, to their generalized equivalent GP and GEV pdfs more recently. We had anticipated that the same evolution would be appropriate for earthquake frequency analysis; however, our results indicate that the more generalized form of the extreme value pdfs do not provide the same advantages for modeling earthquakes as they do for modeling floods. We show that recent developments in regional flood frequency analysis, including the theory of L-moments, hypothesis testing, and parameter estimation [*Hosking and Wallis*, 1997; *Stedinger et al.*, 1993] are valuable statistical tools for modeling earthquake frequency. Seismology and hydrology share several statistical difficulties, most importantly, that the behavior of the upper tail of the distribution is poorly resolved due to the small number of large events. We introduce an index earthquake method, analogous to the index-flood method, for estimating the parameters of the distribution of earthquake magnitudes by pooling data across a set of regions found to behave as a homogeneous super region. The method requires the assumption of a probability distribution and the definition of a homogeneous super region. We use L-moment diagrams and probability plot correlation coefficient hypothesis tests to document that all 45 FE regions are well approximated by a GUM pdf. Using homogeneity tests introduced by *Chowdhury et al.* [1991] and *Hosking and Wallis* [1997], we could not reject the hypothesis that a large portion of the globe (31 FE regions) is homogeneous in terms of all the upper moments of the distribution of earthquake magnitudes. Combining our findings relating to homogeneity and the GUM pdf, we introduce an index earthquake distribution which involves pooling the series of earthquake magnitude from all the individual regions which make up the super region. The resulting index earthquake distribution is a single parameter model that only depends on a region-specific scaling factor, which is the mean earthquake magnitude. The mean earthquake magnitude can be estimated from recorded local seismicity or from physical models.

[40] In flood frequency analysis, it is rare to be able to accept the hypothesis of homogeneity even for a small geographic region (for example, an entire state), so the degree of spatial homogeneity reported in Table 1 and Figure 3 for earthquake magnitudes across broad regions of the globe is striking and warrants further research. Future research on the series of annual maximum earthquakes should further address the issue of censoring due to lack of observations below the magnitude of completeness.

Appendix A: Probability Distribution for Extreme Events

[41] This section provides a summary of some of the most commonly used probability distributions in flood frequency analysis which are shown here to be useful in earthquake frequency analysis for both POT and AM series of earthquake magnitudes.

A1. Peaks Over Threshold Series

[42] The distribution of earthquake magnitudes m, have long been assumed to follow the power law model given by *Gutenberg and Richter* [1954] which we term the GR model

$$\log_{10}(N) = a - bm \tag{A1}$$

where N is the number of earthquakes which have exceeded magnitude m, and a and b are constants. The equivalent pdf corresponding to the GR model in (A1) is the EXP pdf

$$f_{EXP}(m) = \beta \exp[-\beta(m - m_o)] \quad \text{for} \quad m_o < m < \infty \quad \text{and} \quad \beta > 0 \tag{A2}$$

where $\beta = b \ln(10)$ and m is the observed earthquake magnitude in excess of some minimum threshold level m_o [*Kijko and Graham*, 1998; *Utsu*, 1999]. The GR model in equation (A1) is equivalent to the EXP pdf in equation (A2) with mean, variance, skew, and kurtosis of earthquake magnitudes given by

$$\mu_{\text{EXP}} = m_0 + [1/\beta] \tag{A3}$$

$$\sigma^2_{\text{EXP}} = 1/\beta^2 \tag{A4}$$

$$\gamma_{\text{EXP}} = 2 \tag{A5}$$

$$\text{K}_{\text{EXP}} = 9 \tag{A6}$$

The quantile function for an EXP pdf is needed for constructing probability plots and estimating earthquake magnitudes corresponding to a recurrence interval and is given by

$$m_{\text{EXP}}(p) = \frac{\beta m_o - \ln(1-p)}{\beta} \tag{A7}$$

where p is the nonexceedance probability given by the cumulative density function (cdf) $p = F_{\text{EXP}}(m) = P[M \le m]$.

[43] The GP model [*Pickands*, 1975] is a generalization of the EXP model for earthquake POT series, and is given by

$$f_{\text{GP}}(m) = \beta[1 - \kappa\beta(m - m_o)]^{\left(\frac{1}{\kappa}\right)-1} \quad \text{for } m_o < m < \infty \quad \beta > 0 \quad \kappa \neq 0 \tag{A8}$$

where β and κ are scale and shape parameters, respectively, and β is the same as in the EXP pdf. The EXP pdf in equation (A2) is a special case of the GP model because equation (A8) reduces to equation (A2) when the shape parameter $\kappa = 0$. For the GP model in equation (A8) the bounds on m are

$$m_o \le m \le m_o + [1/(\beta\kappa)] \qquad \text{for } \kappa > 0 \tag{A9}$$

$$m_o + [1/(\beta\kappa)] \le m \le \infty \quad \text{for} \quad \kappa < 0 \tag{A10}$$

hence an upperbound on the distribution of m implies that $\kappa > 0$. Due to sample variability, it is quite possible for sample estimates of κ, based on small samples, to be negative. For the GP model in equation (A8), *Hosking and Wallis* [1987] report the mean, variance, skew, and kurtosis:

$$\mu_{\text{GP}} = m_o + \frac{1}{\beta(1+\kappa)} \tag{A11}$$

$$\sigma^2_{\text{GP}} = \frac{1}{\beta^2\left[(1+\kappa)^2(1+2\kappa)\right]} \tag{A12}$$

$$\gamma_{\text{GP}} = \frac{2(1-\kappa)(1+2\kappa)^{1/2}}{(1+3\kappa)} \tag{A13}$$

$$\text{K}_{\text{GP}} = \frac{3(1+2\kappa)(3-\kappa+2\kappa^2)}{(1+3\kappa)(1+4\kappa)} - 3. \tag{A14}$$

Note that the rth moment of a GP pdf only exists for $\kappa > (-1/r)$ whereas L-moments always exist. For example, the skew coefficient only exists for $\kappa > -1/3$. The quantile function for the GP pdf is given by

$$m_{\text{GP}}(p) = \frac{1 + \kappa\beta m_o - (1-p)^\kappa}{\kappa\beta} \tag{A15}$$

where p is the nonexceedance probability. A complete analysis of the properties and parameter estimation methods for the GP distribution is provided by *Hosking and Wallis* [1987], *Rosbjerg et al.* [1992], and *Embrechts et al.* [1997]. It has previously been applied in modeling large insurance claims, as a failure-time distribution in reliability studies, and in problems where the EXP pdf might be used but some robustness is required against heavier tailed or lighter tailed alternatives [*Hosking and Wallis*, 1987].

A2. Annual Maximum Series

[44] When arrivals of earthquakes are assumed to follow a Poisson process, the EXP model for the POT series is equivalent to the GUM type I extreme value model for the AM series. The cdf of a GUM variable is

$$F_{\mathrm{GUM}}(m) = \exp[-\exp(-\beta(m-\xi))] \qquad m_o < m < \infty \quad \text{(A16)}$$

where ξ is now the lower bound of the AM series which differs from the threshold m_o of the POT series. Here the scale parameter β in equation (A16) is identical to the scale parameter β in the EXP model given in equation (A2). Hence the scale parameter β of the GUM distribution can be estimated from either the POT or the AM series. *Stedinger et al.* [1993] derive the relationship between the GUM model for the AM series and the EXP model of the POT series. They show that if λ is the average number of exceedances per year of an earthquake of magnitude m_o then the lower bound ξ in the GUM model is related to the lower bound m_o in the EXP or GR model via

$$\xi = m_o + \frac{\ln(\lambda)}{\beta}. \quad \text{(A17)}$$

The GUM distribution has mean, variance, skewness, and kurtosis given by

$$\mu_{\mathrm{GUM}} = \xi + (0.5772/\beta) \quad \text{(A18)}$$

$$\sigma^2_{\mathrm{GUM}} = \frac{\pi^2}{6\beta^2} \quad \text{(A19)}$$

$$\gamma_{\mathrm{GUM}} = 1.1396 \quad \text{(A20)}$$

$$\mathrm{K}_{\mathrm{GUM}} = 5.4 \quad \text{(A21)}$$

Like the EXP/GR models for the POT series, the key shortcomings of use of the GUM model for modeling AM series are due to its fixed skew and kurtosis and lack of an upperbound. The quantile function of a GUM pdf is given by

$$m_{\mathrm{GUM}}(p) = \xi - \frac{\ln[-\ln(p)]}{\beta}. \quad \text{(A22)}$$

Stedinger et al. [1993] summarize other properties of the GUM distribution.

[45] The GEV distribution is a generalization of Gumbel's type I, II, and III distributions and was introduced by *Jenkinson* [1969] to hydrology and by *Makjanić* [1980, 1982] to seismology and is summarized by *Stedinger et al.* [1993]. The cdf of a GEV distribution is given by

$$F_{\mathrm{GEV}}(m) = \exp\left[-(1-\kappa\beta^*(m-\xi))^{1/\kappa}\right] \quad \text{for } \kappa \neq 0 \quad \text{(A23)}$$

where here the shape parameter κ is identical to the shape parameter of the GP distribution given in equation (A8), hence κ can be estimated from either the POT or AM series. Like the GP model in equation (A8), the GEV model has an upperbound when $\kappa > 0$ so that

$$\xi \le m \le \xi + \lfloor 1/(\beta^*\kappa) \rfloor \quad \text{for } \kappa > 0 \quad \text{(A24)}$$

$$\xi + \lfloor 1/(\beta^*\kappa) \rfloor \le m \le \infty \quad \text{for } \kappa < 0 \quad \text{(A25)}$$

Analogous to equation (A17) for the GUM distribution, *Stedinger et al.* [1993] show that the lower bound ξ and scale parameter β^* in the GEV model is related to the lower bound m_o in the GP model via the following relations

$$\xi = m_o + \frac{1-\lambda^{-\kappa}}{\kappa\beta} \quad \text{(A26)}$$

$$\beta^* = \beta\lambda^{\kappa} \quad \text{(A27)}$$

where again, λ is the average number of exceedances per year of an earthquake of magnitude m_o. For $\kappa > -1/3$ the mean, variance and skew of a GEV variable are given by

$$\mu_{\mathrm{GEV}} = \xi + \frac{[1-\Gamma(1+\kappa)]}{\kappa\beta^*} \quad \text{(A28)}$$

$$\sigma^2_{\mathrm{GEV}} = \frac{\left[\Gamma(1+2\kappa) - \{\Gamma(1+\kappa)\}^2\right]}{\kappa^2\beta^{*2}} \quad \text{(A29)}$$

$$\gamma_{\mathrm{GEV}} = \mathrm{sgn}(\kappa)\frac{-\Gamma(1+3\kappa) + 3\Gamma(1+\kappa)\Gamma(1+2\kappa) - 2\Gamma^3(1+\kappa)}{\left[\Gamma(1+2\kappa) - \Gamma^2(1+\kappa)\right]^{3/2}} \quad \text{(A30)}$$

where sgn( ) is the sign function, and $\Gamma(\ )$ is the gamma function. The quantile function of a GEV variable is given by

$$m_{\mathrm{GEV}}(p) = \xi + \frac{[1-(-\ln(p))^{\kappa}]}{\kappa\beta^*} \quad \text{(A31)}$$

Appendix B: Parameter Estimation

B1. Peaks Over Threshold Series Estimators

[46] Assuming that a POT times series of earthquake magnitudes m_i for $i = 1,\ldots,n$ is available with $m_i \ge m_o$ for all $i = 1,\ldots,n$ where n is the sample size. Sample estimates of the mean $\overline{m}$ and standard deviation s are given by

$$\overline{m} = \frac{1}{n}\sum_{i=1}^{n} m_i \quad \text{and} \quad s = \sqrt{\frac{1}{n}\sum_{i=1}^{n}(m_i - \overline{m})^2} \quad \text{(B1)}$$

In all cases, for the POT series, the lower bound m_o is simply the threshold used in defining the POT series. Solving the expression for the mean of an EXP variable in equation (A3) for β leads to

$$\hat{\beta} = \frac{1}{\overline{m} - m_o} \quad \text{and} \quad \hat{b} = \frac{1}{(\overline{m} - m_o)\ln(10)}. \tag{B2}$$

Combining the moment equations for the mean and variance of a GP variable in equations equations (A11) and (A12) leads to the following MM sample estimators for κ and β:

$$\hat{\beta} = \frac{1}{(\overline{m} - m_o)(1 + \hat{\kappa})} \quad \text{and} \quad \hat{\kappa} = \frac{1}{2}\left[\frac{\overline{m} - m_o}{s} - 1\right] \tag{B3}$$

where m_o is the assumed threshold which defines the POT series. Note that the GR/EXP model is a special case of the GP model when $\kappa = 0$, so the estimators for $\hat{\beta}$ in equations (B2) and (B3) are equivalent when $\kappa = 0$.

[47] The POT series can also be used to estimate parameters of either the GUM or GEV models. For the GUM pdf, the scale parameter β is identical to β in the EXP pdf, hence it can be estimated from equation (B2). The lower bound ξ can be estimated from equation (A17) by using m_o equal to the chosen threshold of the POT series, and with an estimate of λ as simply the average number of events above the threshold m_o in the POT series. For the GEV pdf, the estimator of κ for the GP pdf given in equation (B3) can also be used to estimate the value of κ in the GEV pdf. The other two parameters of the GEV pdf, ξ and β^* can then be estimated from equations (A26) and (A27), respectively, by using m_o equal to the chosen threshold of the POT series, the value of $\hat{\beta}$ from equation (B3) and again, with an estimate of λ as simply the average number of events above the threshold m_o in the POT series.

B2. Annual Maximum Series Estimators

[48] Assume that a complete AM series of earthquake magnitudes m_i $i = 1,\ldots,n$ is available where n is the record length in years. Sample estimates of the mean and standard deviation s are identical to those for the POT series in equation (B1), but with m_i now equal to the AM earthquake magnitude in year i. Unlike the models for the POT series which all had a lower bound of m_o, the AM series have a lower bound ξ which differs from m_o.

[49] For the GUM model, method of moments estimates of the scale and lower bound parameters are obtained from equations (A18) and (A19) which leads to

$$\hat{\beta} = \frac{\pi}{s\sqrt{6}} \tag{B4}$$

$$\hat{\xi} = \overline{m} - \frac{0.5772}{\hat{\beta}}. \tag{B5}$$

For the GEV model, a MM estimate of the shape parameter κ is obtained by substitution of sample skewness $\hat{\gamma}_m$ computed from

$$\hat{\gamma}_m = \frac{\frac{1}{n}\sum_{i=1}^{n}(m_i - \overline{m})^3}{s^3} \tag{B6}$$

in place of the true skew γ_{GEV} in equation (A30) and then solving equation (A30) for $\hat{\kappa}$ using a numerical search. Note that in general, the values of γ_{GEV} are inversely proportional to values of κ and good initial values for starting the search are given for the special case when the GEV pdf reduces to the GUM pdf (i.e., $\gamma_{GEV} = 1.14$ and $\kappa = 0$). The location and scale parameters can be estimated from equations (A28) and (A29) which leads to

$$\hat{\beta}^* = \mathrm{sgn}(\hat{\kappa})\frac{\sqrt{\Gamma(1 + 2\hat{\kappa}) - \Gamma(1 + \hat{\kappa})^2}}{\hat{\kappa}s} \tag{B7}$$

$$\hat{\xi} = \overline{m} - \frac{1 - \Gamma(1 + \hat{\kappa})}{\hat{\kappa}\hat{\beta}^*}. \tag{B8}$$

[50] **Acknowledgments.** We thank two anonymous reviewers for their thoughtful and thorough review comments which led to significant improvements to our original manuscript. We are also indebted to Jery R. Stedinger, for his guidance on estimation of the variance of an *L*-moment estimator of L–C_v for the Gumbel distribution.

References

Asquith, W. H. (2006), lmomco: L-moments, Trimmed L-moments, L-comoments, and Many Distributions, R package version 0.82.

Beirlant, J., Y. Goegebeur, J. Teugels, J. Segers, D. DeWaal, and C. Ferro (2005), *Statistics of Extremes Theory and Applications*, 490 p, John Wiley, Hoboken, N. J.

Bobee, B., and P. F. Rasmussen (1995), Recent advances in flood frequency analysis, *Rev. Geophys.*, *33*, 1111–1116.

Bommer, J. J., et al. (2004), The challenge of defining upper bounds on earthquake ground motions, *Seismol. Res. Lett.*, *75*(1), 82–95.

Cheng, E., and C. Yeung (2002), Generalized extreme gust wind speeds distributions, *J. Wind Eng. Ind. Aerodyn.*, *90*(12-15), 1657–1669.

Chowdhury, J. U., J. R. Stedinger, and L.-H. Lu (1991), Goodness-of-fit tests for regional generalized extreme value flood distributions, *Water Resour. Res.*, *27*(7), 1765–1776.

Christopeit, N. (1994), Estimating parameters of an extreme value distribution by the method of moments, *J. Stat. Plan. Inference*, *41*, 173–186.

Cosentino, P., V. Ficarra, and D. Luzio (1977), Truncated exponential frequency-magnitude relationship in earthquake statistics, *Bull. Seismol. Soc. Am.*, *67*(6), 1615–1623.

Cunnane, C. (1989), Statistical distributions for flood frequency analysis, Operational Hydro. Rep. No. 33, World Meteorological Org. (WMO) Geneva, Switzerland.

Cunnane, C. (2004), Unbiased plotting positions–A review, *J. Hydrol.*, *37*, 205–222.

Dalrymple, T. (1960), Flood frequency analysis, Water Supply Paper 1543-A, U.S. Geological Survey, Reston, VA.

Dargahi-Noubary, G. R. (1986), A method for predicting future large earthquakes using extreme order statistics, *Phys. Earth Planet. Inter.*, *42*, 241–245.

Ekström, G., A. M. Dziewonski, N. N. Maternovskaya, and M. Nettles (2005), Global seismicity of 2003: Centroid–moment-tensor solutions for 1087 earthquakes, *Phys. Earth Planet. Inter.*, *148*, 327–351.

Embrechts, P., C. P. Kluppelberg, and T. Mikosh (1997), *Modelling Extremal Events*, 645 p, Spinger, New York.

Epstein, B., and C. Lomnitz (1966), A model for the occurrence of large earthquakes, *Nature*, *211*, 954–956.

Fill, H. D., and J. R. Stedinger (1995), Homogeneity tests based upon Gumbel distribution and a critical appraisal of Dalrymple's test, *J. Hydrol.*, *166*, 81–105.

Filliben, J. J. (1975), The probability plot correlation coefficient test for normality, *Technometrics*, *17*(1), 111–117.

Gringorten, I. I. (1963), A plotting rule for extreme probability paper, *J. Geophys. Res.*, *68*(3), 813–814.

Gumbel, E. J. (1958), *Statistics of Extremes*, 375 p, Columbia Univ. Press, New York.

Gutenberg, B., and C. F. Richter (1954), *Seismicity of the Earth*, Princeton Univ. Press, Princeton, N. J.

Hosking, J. R. M. (1990), L-moments: Analysis and estimation of distributions using linear combinations or order statistics, *J. R. Stat. Soc., Ser. B*, *52*, 105–124.

Hosking, J. R. M. (1998), "L-Moments", in *Encyclopedia of Statistical Sciences*, update vol. 2, edited by S. Kotz, C. Read, and D. L. Banks, pp. 357–362, John Wiley, Hoboken, N. J.

Hosking, J. R. M., and J. R. Wallis (1987), Parameter and quantile estimation for the generalized Pareto distribution, *Technometrics*, *29*(3), 339–349.

Hosking, J. R. M., and J. R. Wallis (1997), *Regional Frequency Analysis: An Approach Based on Lmoments*, Cambridge Univ. Press, New York.

Howell, B. F. (1985), On the effect of too small a data base on earthquake frequency diagrams, *Bull. Seismol. Soc. Am.*, *75*(4), 1205–1207.

Jenkinson, A. F. (1969), "Statistics of Extremes", in *Estimation of Maximum Floods*, WMO No. 233, TP 126, (Technical note no. 98), pp. 183–228.

Kagan, Y. Y. (1993), Statistics of characteristic earthquakes, *Bull. Seismol. Soc. Am.*, *83*(1), 7–24.

Kagan, Y. Y. (1997), Seismic moment-frequency relation for shallow earthquakes: Regional comparison, *J. Geophys. Res.*, *102*(B2), 2835.

Kanamori, H. (1977), Energy-release in great earthquakes, *J. Geophys. Res.*, *82*(20), 2981–2987.

Kijko, A., and G. Graham (1998), Parametric-historic procedure for probabilistic seismic hazard analysis: Part I. Estimation of maximum regional magnitude m_{max}, *Pure Appl. Geophys.*, *152*, 413–442.

Leese, M. N. (1973), Use of censored data in the estimation of Gumbel distribution parameters for the annual maximum flood series, *Water Resour. Res.*, *9*(6), 1534–1542.

Livezey, R. E., and W. Y. Chen (1983), Statistical field significance and its determination by Monte Carlo techniques, *Mon. Weather Rev.*, *111*, 46–59.

Lombardi, A. M. (2003), The maximum likelihood estimator of b-value for mainshocks, *Bull. Seismol. Soc. Am.*, *93*(5), 2082–2088.

Ma, Q. S., Y. B. Li, and J. Li (2006), Regional frequency analysis of significant wave heights based on L-moments, *China Ocean Eng.*, *20*(1), 85–98.

Madsen, H., P. F. Rasmussen, and D. Rosbjerg (1997), Comparison of annual maximum series and partial duration series methods for modeling extreme hydrologic events: 1. At-site modeling, *Water Resour. Res.*, *33*(4), 747–758.

Main, I. (1996), Statistical physics, seismogenesis, and seismic hazard, *Rev. Geophys.*, *34*(4), 433–462.

Main, I. (2000), Apparent breaks in scaling in the earthquake cumulative frequency-magnitude distribution: Fact or artifact?, *Bull. Seismol. Soc. Am.*, *90*(1), 86–97.

Makjanić, B. (1980), On the frequency distribution of earthquake magnitude and intensity, *Bull. Seismol. Soc. Am.*, *70*(6), 2253–2260.

Makjanić, B. (1982), On the generalized exponential distribution of the earthquake intensity and magnitude, *Bull. Seismol. Soc. Am.*, *72*(3), 981–986.

Onibon, H., T. B. M. J. Ouarda, M. Barbet, A. St-Hiliare, B. Bobee, and P. Bruneau (2004), Regional frequency analysis of annual maximum daily precipitation in Quebec, Canada, *Hydrol. Sci. J.*, *49*(4), 717–735.

Pacheco, J. F., C. H. Scholz, and L. R. Sykes (1992), Changes in frequency-size relationship from small to large earthquakes, *Nature*, *355*, 71–73.

Pickands, J. (1975), Statistical inference using extreme order statistics, *Ann. Stat.*, *3*, 119–131.

Pisarenko, V. K., and D. Sornette (2003), Characterization of the frequency of extreme earthquake events by the generalized Pareto distribution, *Pure Appl. Geophys.*, *160*, 2343–2364.

Potter, K. W. (1987), Research on flood frequency analysis: 1983–86, *Rev. Geophys.*, *25*(2), 113–118.

R Development Core Team (2006), R: A language and environment for statistical computing, R Foundation for statistical computing, Vienna, Austria.

Ribatet, M. (2005), RFA: Regional Frequency Analysis, R package version 0.0-6.

Rosbjerg, D., H. Madsen, and P. F. Rasmussen (1992), Prediction in partial duration series with generalized Pareto-distributed exceedances, *Water Resour. Res.*, *28*(11), 3001–3010.

Schorlemmer, D., S. Wiemer, and M. Wyss (2005), Variations in earthquake-size distribution across different stress regimes, *Nature*, *437*, 539–542.

Stedinger, J. R., R. M. Vogel, and E. Foufoula-Georgiou (1993), Frequency Analysis of Extreme Events, Chapter 18, *Handbook of Hydrology*, McGraw-Hill, New York, David R. Maidment, Editor-in-Chief.

Stein, S., and A. Newman (2004), Characteristic and uncharacteristic earthquakes as possible artifacts: Application to the New Madrid and Wabash seismic zones, *Seismol. Res. Lett.*, *75*(2), 173–187.

Utsu, T. (1999), Representation and analysis of the earthquake size distribution: A historical review and some new approaches, *Pure Appl. Geophys.*, *155*, 509–535.

Vogel, R. M. (1986), The probability plot correlation coefficient test for the normal, log normal and Gumbel distributional hypotheses, *Water Resour. Res.*, *22*(4), 587–590.

Vogel, R. M., and N. M. Fennessey (1993), L-moment diagrams should replace product-moment diagrams, *Water Resour. Res.*, *29*(6), 1745–1752.

Vogel, R. M., and I. Wilson (1996), Probability distribution of annual maximum, mean, and minimum streamflows in the United States, *J. Hydrol. Eng.*, *1*(2), 69–78.

Young, J. B., B. W. Presgrave, H. Aichele, D. A. Wiens, and E. A. Flinn (1996), The Flinn-Engdahl regionalisation scheme: The 1995 revision, *Phys. Earth Planet. Inter.*, *96*(4), 223–297.

Youngs, R. R., and K. J. Coppersmith (1985), Implications of fault slip and earthquake recurrence models to probabilistic seismic hazards estimates, *Bull. Seismol. Soc. Am.*, *75*(4), 939–964.

L. G. Baise, E. M. Thompson, and R. M. Vogel, Department of Civil and Environmental Engineering, Tufts University, Medford, MA, USA. (eric.thompson@tufts.edu)